THE ASTROPHYSICAL JOURNAL, 513:L143–L146, 1999 March 10

SEISMIC IMAGES OF A SOLAR FLARE

A.-C. DONEA[1]
Astronomical Institute of the Romanian Academy, Cutitul de Argint 5, RO-75212, Bucharest, Romania
AND
D. C. BRAUN[2] AND C. LINDSEY
Solar Physics Research Corporation, 4720 Calle Desecada, Tucson, AZ 85718
Received 1998 September 28; accepted 1998 December 29; published 1999 February 18

ABSTRACT

We have used helioseismic holography to render seismic images of the solar flare of 1996 July 9, whose helioseismic signature was recently reported by Kosovichev & Zharkova. We computed time series of "egression power maps" in 2 mHz bands centered at 3.5 and 6 mHz. These images suggest an oblong acoustic source associated with the flare some 18 Mm in the north-south direction and approximately 15 Mm in the east-west direction. The considerable preponderance of the flare acoustic power emanates in the 3.5 mHz band. However, because the ambient noise in the 6 mHz band is much lower and the diffraction limit for 6 mHz waves is much finer, the flare is rendered far more clearly in the 6 mHz band. The 6 mHz flare signature lags the 3.5 mHz by approximately 4 minutes.

Subject headings: Sun: flares — Sun: oscillations — sunspots

1. INTRODUCTION

Solar flares are probably the most spectacular local phenomena at the solar surface, often releasing large fluxes of X-rays and energetic particles. Kosovichev & Zharkova (1998a) recently reported the first clear acoustic signature of a solar flare in observations from the Michelson Doppler Imager (MDI) from the *Solar and Heliospheric Observatory* (*SOHO*). Their analysis rendered a significant circular wave packet emanating from the event of 1996 July 9, in NOAA Active Region 7978, during the time when the Sun was at activity minimum. This event (classified as X2.6/lB) was the only significant flare of moderate size to appear in 1996. The Burst and Transient Source Experiment (BATSE) from the *Compton Gamma-Ray Observatory* detected an X-ray flux in the energy range 25–100 keV beginning at 09:07:40 UT and reaching a maximum after 2 minutes. The MDI Doppler images show a compact, equally impulsive redshift that reaches maximum approximately 1 minute after the X-ray peak.

Kosovichev & Zharkova (1998a) show a circular wave packet emanating from the flare, extending horizontally some 120 Mm from the location of the flare, up to 55 minutes after the impulsive phase of the flare. This wave packet, which they liken to surface ripples on a pond after a stone has been tossed into it, is the signature of an acoustic disturbance that has penetrated tens of megameters beneath the solar photosphere before refracting back to the surface.

Helioseismic holography is a general diagnostic intended for local helioseismology, based on the concept of seismic imaging. It was introduced and developed conceptually by Lindsey & Braun (1990), Braun et al. (1992), and Lindsey & Braun (1997) as a means of imaging acoustic sources in the solar interior and far side. Roddier (1975) proposed the technique previously. It has been applied by Chang et al. (1997) and Chen et al. (1998) to helioseismic observations from the TON network. It has been applied likewise to the *SOHO*-MDI observations by Braun et al. (1998) and Lindsey & Braun (1998a, 1998b, 1999) to render images of conspicuous "acoustic moats" surrounding all well-developed sunspots, remarkable acoustic "condensations" more than 10 Mm beneath the photospheres of large active regions (Lindsey & Braun 1998b; Braun & Lindsey 1999), and "acoustic glories," extended 5–6 mHz acoustic egression power halos surrounding active regions (Braun & Lindsey 1999; Donea, Lindsey, & Braun 1999). In this study, we have applied the technique to the flare signature reported by Kosovichev & Zharkova (1998a) to render a coherent spatial representation of the acoustic source of the observed disturbance.

2. THE ACOUSTIC ANALYSIS

The application of helioseismic holography to the flare of 1996 July 9 is a straightforward variation of the technique described by Lindsey & Braun (1997). The medium-resolution MDI Dopplergrams are 1024 × 1024 pixel images made with a cadence of 60 s and averaged over approximately this time. The observed surface acoustic field $\psi(\boldsymbol{r}', t')$ is propagated in time reverse from its horizontal location and time $(\boldsymbol{r}', t')$ to a location and time $(\boldsymbol{r}, z, t)$ at depth z by convolution with a Green's function G_+ to render a regressed acoustic field, which we call the egression:

$$H_+(z, \boldsymbol{r}, t) = \int dt' \int_{a<|\boldsymbol{r}-\boldsymbol{r}'|<b} d^2\boldsymbol{r}'\, G_+(z, \boldsymbol{r}, t, \boldsymbol{r}', t')\, \psi(\boldsymbol{r}', t'). \quad (1)$$

In our case, the computation is made over an annular acoustic pupil of inner radius $a = 15.3$ Mm and outer radius $b = 44.5$ Mm. The surface is assumed to be a perfect absorber, and so the Green's function is truncated after a single skip to the surface. The computation expressed by equation (1), then coherently regresses the acoustic field a single skip, from the observed surface disturbance to the surface point at which it is supposed to have originated. Since all of the egressions imaged in this study are computed at the surface ($z = 0$), we omit the depth z in the following discussion.

[1] Also at National Solar Observatory, Tucson, AZ.
[2] Mailing address: High-Altitude Observatory, National Center for Atmospheric Research, P.O. Box 3000, Boulder, CO 80307-3000. The National Center for Atmospheric Research is sponsored by the National Science Foundation.

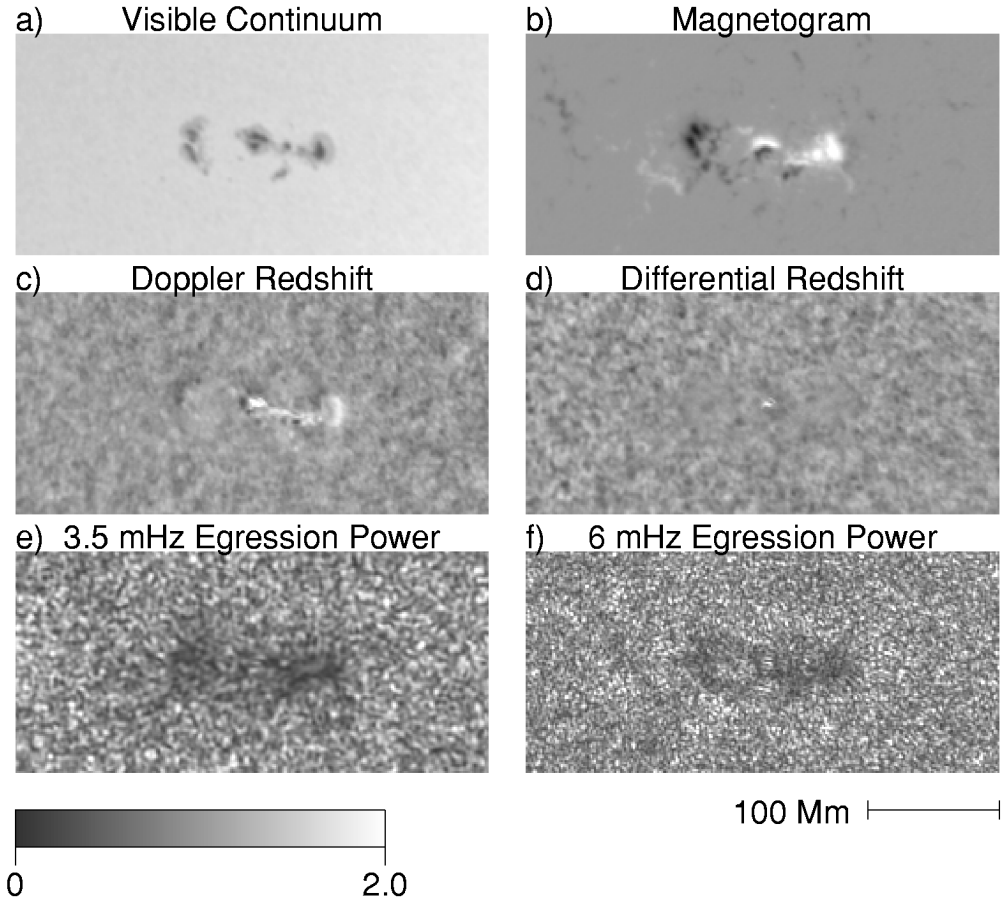

FIG. 1.—Egression power maps at 3.5 and 6 mHz are compared with (*a*) a continuum image of the Sun and (*b*) a magnetogram taken by the *SOHO*-MDI instrument at 01:05 and 16:04 UT, respectively. (*c*) MDI Dopplergram imaging the redshift at 09:11 UT, the moment of maximum redshift, ~1.5 km s^{-1}, at the flare location. (*d*) Difference between the Dopplergram in panel *c* and the Dopplergram made 2 minutes earlier, before the signature of the flare was apparent in the Dopplergrams. (*e*, *f*) Egression power maps integrated over the 2.1 hr interval beginning at 08:06 UT in 2 mHz bands centered at 3.5 and 6 mHz, respectively. The gray scale at the bottom applies to the egression power maps, both normalized to unity for the mean quiet Sun in their respective frequency bands.

For the purpose of considerably improved numerical efficiency, the computation was made in the "spectral perspective" described by Lindsey & Braun (1997), which directly renders the temporal Fourier transform $\hat{H}_+(\boldsymbol{r}, \nu)$ of $H_+(\boldsymbol{r}, t)$, such that

$$H_+(\boldsymbol{r}, t) = \int_{-\infty}^{\infty} d\nu \, e^{2\pi i \nu t} \, \hat{H}_+(\boldsymbol{r}, \nu). \quad (2)$$

In this study, a complex variant of the egression expressed above is obtained by computing the above integral only over a selected positive frequency band, $\Delta\nu = 2$ mHz, that is centered at 3.5 mHz in one case and at 6 mHz in another. The egression power in either band is simply the real modulus of the resulting complex amplitude:

$$P(\boldsymbol{r}, t) = |H_+(\boldsymbol{r}, t)|^2. \quad (3)$$

The restriction to a limited frequency band is accomplished at a significant expense in temporal resolution: $\Delta t = 1/\Delta\nu = 500$ s, in accordance with the Heisenberg principle.

The use of equation (7) in Lindsey & Braun (1997),

$$G_+(z, \boldsymbol{r}, t, \boldsymbol{r}', t') = \delta\,[t - t' - T(|\boldsymbol{r} - \boldsymbol{r}'|, z)]\; f(|\boldsymbol{r} - \boldsymbol{r}'|, z), \quad (4)$$

to express the Green's function neglects *dispersion*, which is important for temporal discrimination. For the purpose of this study, these phase errors were measured by comparing the local wave amplitude in the quiet Sun with the egression as a function of frequency, and the Green's function was corrected accordingly. However, amplitude-egression phase maps of active regions suggest that the active region subphotosphere and acoustic moat can introduce temporal errors up to ~1 minute.

Figure 1 shows egression power maps of NOAA AR 7978 integrated over a period of 2.1 hr that includes the flare, compared with other diagnostic images of NOAA AR 7978. Figure 1*a* shows a *SOHO*-MDI continuum image, and Figure 1*b* shows a *SOHO*-MDI magnetogram. Figure 1*c* shows an MDI Dopplergram at 09:11 UT, the time of maximum redshift at the center of the flare. In this representation, redshift is indicated by a lighter tone and blueshift is indicated by a darker tone. Figure 1*d* shows the difference between this Dopplergram and that which the MDI instrument obtained 2 minutes before. This shows the compact redshift at the center of the flare partially surrounded by a diffuse blueshift. Figures 1*e* and 1*f* show egression power maps of these regions in 2 mHz bands centered at 3.5 and 6.0 mHz respectively, integrated over the 2.1 hr period 08:06–10:13 UT. The 3.5 mHz egression power map (Fig. 1*e*) clearly shows the acoustic absorption profile of sunspots em-

bedded in the active region and the encompassing acoustic moat. The 6 mHz egression power map (Fig. 1*f*) also shows the conspicuous egression power halo surrounding all large active region complexes that Braun & Lindsey (1999) and Donea et al. (1999) call the acoustic glory.

Figure 2 shows egression power snapshots of NOAA AR 7978 at a sampling of times during the flare, again over bandwidths of 2 mHz. The left-hand column shows egression power images centered at 3.5 mHz at the same times as the images in the right-hand column, which are centered at 6.0 mHz. The top frame in each column shows the egression power integrated over a 2 hr period beginning at 08:06 UT (see also Figs. 1*e* and 1*f*, respectively). The underlying frames show the egression power sampled over an interval of 20 minutes, over which time the flare signature emerges in both frequency bands and disappears. The acoustic signatures of the solar flare at both frequencies are easily visible in the centers of the frames representing the time interval from 09:05 to 09:19 UT.

The peak of the 3.5 mHz signature occurs ~3 minutes before the maximum Doppler redshift signature of the flare at 9:11 UT (seen in Fig. 1*c*). The appearance of a significant acoustic signature in these frames minutes before the maximum X-ray signature recorded by BATSE, at approximately 09:10 UT, should not be mistaken for an acoustic precursor of the flare. This can probably be explained by temporal dispersion due to truncation of the acoustic spectrum of the *SOHO*-MDI observations to a 2 mHz bandwidth, combined with phase errors introduced by the active region subphotosphere. Phase measurements by Braun (1995) and later temporal correlation measurements by Duvall et al. (1996) and Braun (1997) suggest sound-transit times in sunspot subphotospheres 60 s shorter than in the quiet Sun for outgoing waves.

Both the 3.5 and 6 mHz flare egression signatures are extended spatially, approximately 18 Mm in the north-south direction and 15 Mm in the east-west direction. This is much greater than the differential signature shown directly by the MDI Dopplergrams themselves (see Kosovichev & Zharkova 1998a, 1998b; also Fig. 1*d*, above). The differential Doppler signature is extended rather more in the east-west direction than in the north-south direction. The acoustic signatures are securely encompassed by the penumbra of the bipolar sunspot that marks the center of the active region. In fact, the flare signature is centered on the magnetic boundary separating the positive polarity of the northern sunspot umbra from the southern umbra. The fine structures of the 3.5 and 6 mHz signatures differ considerably. Both seem to be composed of horizontally oriented kernels whose vertical widths define the diffraction limit of the holographic images, 5.6 and 3.3 Mm at 3.5 and 6 mHz, respectively. The geometry of the acoustic images in terms of horizontally oriented kernels stacked in the vertical dimension suggests a source that is temporally coherent in the east-west direction with a strong temporal dependence along the north-south direction, which would give rise to phase interference to explain the horizontal nodes that modulate the image in the north-south direction.

The 3.5 mHz egression signature of the flare has a half-power duration of 8 minutes, approximately the 500 s temporal resolution corresponding to the bandwidths of the computations. This suggests that the raw flare signature, untruncated in temporal frequency, could be significantly shorter, indeed impulsive. However, the 6 mHz half-power duration is significantly longer than the temporal resolution limit, about 11 minutes. The onset of the 6 mHz egression signature, while it commences at approximately the same time as the 3.5 mHz egression signature, is significantly slower, its peak delayed approximately 4 minutes with respect to the 3.5 mHz peak.

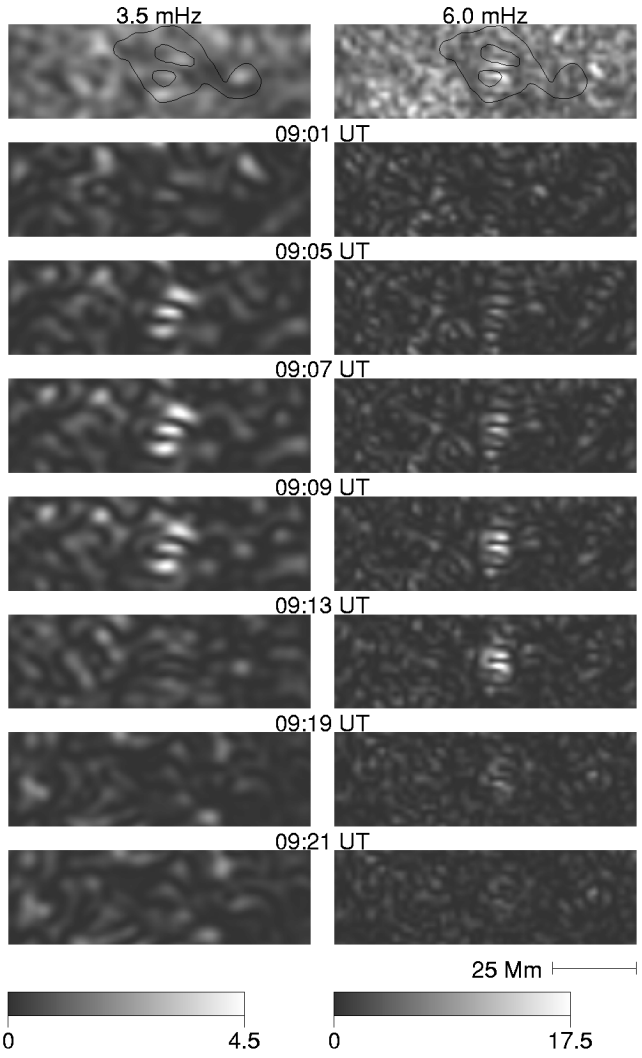

FIG. 2.—Egression power maps are shown at a selection of times covering the occurrence of the flare. *Left column:* Flare egression power signature in a 2 mHz band centered at 3.5 mHz. *Right column:* The same in the 2 mHz band centered at 6.0 mHz. The top frame in each column shows the egression power in the respective frequency band integrated over the 2.1 hr interval beginning at 08:06 UT. These are magnifications of the centers of Figs. 1*e* and 1*f*, respectively. Contours show the locations of the penumbra and enclosed umbras of the bipolar sunspot at the center of the active region. The underlying frames in the left and right columns show the instantaneous egression power at the times indicated above each pair of frames. Gray scales at the bottom apply to the instantaneous egressions, normalized to unity for the mean quiet Sun.

Averaged over the spatial domain of the flare signature, the peak 3.5 mHz egression power of the flare signature is approximately 2.5 times that of the mean quiet Sun. Based on this measurement, we estimate a total acoustic energy of roughly 10^{30} ergs. The corresponding 6 mHz egression power is considerably less, only 1.3% of the 3.5 mHz egression power. However, this small factor is certain to be misleading, since we make no attempt here to account for the modulation transfer function of the MDI instrument (Scherrer et al. 1995), which strongly suppresses the shorter wavelengths that represent the higher frequencies. Without this correction, the mean quiet Sun background in the 6 mHz band is only 0.8% of that at 3.5 mHz. So, the 6 mHz egression power signature, while much

smaller than the 3.5 mHz egression in absolute terms, is approximately 4.1 times that of the 6 mHz mean quiet Sun. In fact, the significance of the flare signature at 6 mHz is further enhanced by its finer resolution, approximately twice that of the 3.5 mHz computations, because of diffraction. This gives the 6 mHz flare signature 4 times the number of area resolution elements of the 3.5 mHz signature. The formidable statistical advantage that accrues to the 6 mHz signature from the considerations stated above is easily overlooked by the reader who fails to compare the gray scales of the 3.5 and 6 mHz egression power images in Figure 2 and take proper account of the higher resolution. In fact, the 6 mHz flare egression power is 17.5 times that of the mean quiet Sun at its peak—by far the most intense acoustic emission in the 6 mHz spectrum—and is clearly recognized in the 2 hr integration shown in Figure 1*f*, while the corresponding 3.5 mHz signature (Fig. 1*e*) is inconspicuous.

3. DISCUSSION AND CONCLUSIONS

Kosovichev & Zharkova (1998b) propose that the acoustic signature of the flare can be understood in terms of a downward-propagating shock such as would result as a hydromechanical reaction to ablation of the solar chromosphere by accelerated particles during the impulsive phase of the flare. This process has been modeled in some detail by Fisher, Canfield, & McClymont (1985a, 1985b, 1985c). The anonymous referee suggests that the considerable spatial extension of the flare signature could be the result of scattering by the bipolar sunspot of acoustic emission from a more compact acoustic source. This possibility needs to be seriously considered. The question may be clarified by comparing acoustic egression signatures of flares with Hα images.

The 4 minute delay of the 6 mHz peak signature after the 3.5 mHz peak is remarkable. As Kosovichev & Zharkova (1998b) point out, phase perturbations by sunspot subphotospheres are significant. However, it is hard to see how these can introduce temporal errors much greater than 1 minute.

The foregoing results offer a highly encouraging assessment of the general diagnostic utility of helioseismic holography in the temporal domain, and for solar flares in particular. The results confirm the existence of a strong acoustic perturbation from a moderately large flare, as reported by Kosovichev & Zharkova (1998a, 1998b). Detailed acoustic studies of such perturbations can be made in both frequency and temporal domains, simultaneously. One expects a broad range of moderate-sized flares to be amenable to this approach as solar activity increases, and much larger flares, with their advantage in signal with respect to ambient acoustic noise, will certainly offer considerably more detailed information than the single example developed here.

While most of the acoustic flux emanating from the 1996 July 9 flare was clearly concentrated in the 3.5 mHz band, the acoustic power at higher frequencies, 6 mHz, was significant, indeed well out of proportion to the ambient acoustic energy at these frequencies. The results presented here add strong reinforcement to the general experience by Lindsey & Braun (1998b) and Braun & Lindsey (1999) that the higher acoustic frequencies, with their finer diffraction limit, offer a utility in acoustic diagnostics that cannot practically be matched by the 3.5 mHz oscillations that have been so fundamental for global helioseismology. It now appears that local acoustic diagnostics is on the verge of opening a broad range of solar research to empirical examination that has heretofore had to remain largely in the realm of theory. This is certain to contribute considerably to our understanding of solar flares.

We greatly appreciate the excellent support our research has received from the *SOHO*-MDI team and the fine quality of the helioseismic data their instrument has given to us. We very much appreciate wave computations made by and consultation with Yuhong Fan. We thank Mark Rast for his conscientious review of the manuscript. We appreciate very useful comments by Alexander Kosovichev and likewise by the anonymous referee. D. C. B., a long-term visitor at the High-Altitude Observatory, is grateful to Michael Knölker and the staff of HAO for their hospitality and support. This research was supported by NSF grants AST-9521637 and AST-9528249 and NASA grants NAGW-97029 and NAG5-7236.

REFERENCES

Braun, D. C. 1995, ApJ, 451, 859
———. 1997, ApJ, 487, 447
Braun, D. C., & Lindsey, C. 1999, ApJ, 513, L79
Braun, D. C., Lindsey, C., Fan, Y., & Fagan, M. 1998, ApJ, 502, 968
Braun, D. C., Lindsey, C., Fan, Y., & Jefferies, S. M. 1992, ApJ, 392, 739
Chang, H.-K., Chou, D.-Y., LaBonte, B.-G., & The TON Team. 1997, Nature, 389, 825
Chen, H.-R., Chou, D.-Y., Chang, H.-K., Sun, M.-T., Yeh, S.-J., LaBonte, B. J., & The TON Team. 1998, ApJ, 501, L139
Donea, A.-C., Lindsey, C., & Braun, D. C. 1999, ApJ, submitted
Duvall, T. L., Jr., D'Silva, S., Jefferies, S. M., Harvey, J. W., & Schou, J. 1996, Nature, 379, 235
Fisher, G. H., Canfield, R. C., & McClymont, A. N. 1985a, ApJ, 289, 414
Fisher, G. H., Canfield, R. C., & McClymont, A. N. 1985b, ApJ, 289, 425
———. 1985c, ApJ, 289, 434
Kosovichev, A. G., & Zharkova, V. V. 1998a, Nature, 393, 317
———. 1998b, in IAU Symp. 185, New Eyes to See Inside the Sun and Stars, ed. F. Deubner, J. Christensen-Dalsgaard, & D. Kurtz (Dordrecht: Kluwer), 191
Lindsey, C., & Braun, D. C. 1990, Sol. Phys., 126, 101
———. 1997, ApJ, 485, 895
———. 1998a, ApJ, 499, L99
———. 1998b, ApJ, 509, L129
———. 1999, ApJ, 510, 494
Roddier, F. 1975, Comptes Rendus Acad. Sci. B, 281, 93
Scherrer, P. H., et al. 1995, Sol. Phys., 162, 129